Optically pumped transport in ferromagnet-semiconductor Schottky diodes (invited)

A. F. Isakovic
School of Physics and Astronomy, University of Minnesota, Minneapolis, Minnesota 55455

D. M. Carr
Department of Chemical Engineering and Materials Science, University of Minnesota, Minneapolis, Minnesota 55455

J. Strand
School of Physics and Astronomy, University of Minnesota, Minneapolis, Minnesota 55455

B. D. Schultz and C. J. Palmstrøm
Department of Chemical Engineering and Materials Science, University of Minnesota, Minneapolis, Minnesota 55455

P. A. Crowell[a)]
School of Physics and Astronomy, University of Minnesota, Minneapolis, Minnesota 55455

Optical pumping is used to generate spin-polarized carriers in epitaxial ferromagnet-GaAs Schottky diodes with $In_yGa_{1-y}As$ quantum wells placed in the depletion region. A strong dependence of the photocurrent on the polarization state of the incident light is observed, and a series of measurements as a function of excitation energy, bias voltage, magnetic field, and excitation geometry are used to distinguish spin-dependent transport from a variety of background effects. The spin polarization of the photocurrent for pumping energies at and above the band gap of GaAs is of order 0.5% or less. Much larger polarization dependence is observed for excitation energies near the quantum well ground state. Although background effects are very large in this regime, the field dependence of the polarization signal for several samples is suggestive of spin-dependent transport. © *2002 American Institute of Physics.* [DOI: 10.1063/1.1455606]

Conventional ferromagnetic metals such as iron or cobalt are in many respects ideal candidates for electrodes in spin transport devices. They have a large (>40%) spin polarization at the Fermi level, and high quality films can be grown on semiconductor surfaces by molecular beam epitaxy (MBE). With the important exception of InAs, interfaces between common semiconductors and the ferromagnetic transition metals form Schottky barriers, with the Fermi level pinned near the middle of the gap at the surface. Although the presence of a barrier is a disadvantage in the design of ordinary linear devices, it provides some distinct advantages in the case of spin transport. For example, the tunneling current through a barrier depends strongly on the spin-polarized density of states at the Fermi level in the metal. In contrast, the spin polarization of currents in low-barrier ohmic contacts is expected to be strongly suppressed by spin relaxation in the metal near the interface.[1,2]

We report in this article on recent experiments on ferromagnet-GaAs Schottky diode structures in which spin-polarized carriers are created in the semiconductor by optical pumping. The ferromagnetic films are Fe and $Fe_{1-x}Co_x$, and an $In_yGa_{1-y}As$ quantum well is placed in the depletion region of each structure to provide a spatially localized source of optically pumped spins in close proximity (<2000 Å) to the metal–semiconductor interface. Our measurements are conducted as a function of magnetic field, bias voltage, photon energy, and excitation geometry. The spin polarization of the photocurrent is less than 1% when the semiconductor is pumped at energies above the band edge with circularly polarized light. Larger polarizations may be achieved when the quantum well ground state is resonantly pumped,[3] although background effects are also larger in this case. We focus in this article on how experimental parameters such as bias voltage, photon energy, and excitation geometry can be used in an effort to isolate spin-dependent transport from the semiconductor into the ferromagnet in the presence of large backgrounds due to magneto-optical effects.

A schematic band diagram of a reverse-biased *n*-type GaAs Schottky diode is shown in Fig. 1 along with two possible transport processes. Process A is due to electrons tunneling from the ferromagnet into unoccupied states in the conduction band of the semiconductor. In principle, the spin polarization of this current will be determined by the polarization of the density of states in the ferromagnet integrated over the energy range $E_F - V_B < E < E_F$, where V_B is the bias voltage and E_F is the Fermi energy. A means for detecting the spin polarization in this case is suggested by recent experiments on all-semiconductor spin injection devices, in which a quantum well was placed in the depletion region of a forward-biased $p-n$ junction.[4–6] The spin state of the injected carriers was determined by the degree of circular polarization of the electroluminescence emitted by the quantum well. The same technique can be used in a Schottky device such as that of Fig. 1 if there is a sufficient supply of minor-

[a)]Electronic mail: crowell@physics.a.umn.edu

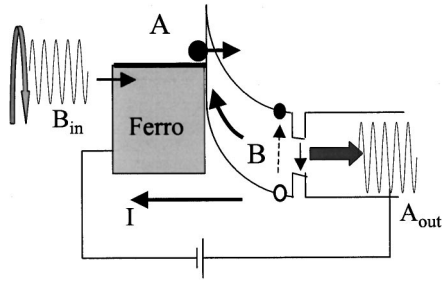

FIG. 1. A schematic depiction of a reverse-biased *n*-type ferromagnetic metal-GaAs Schottky diode. The spin *injection* process (A) occurs by tunneling and can in principle be probed by measuring the polarization state of the light emitted by recombination in the quantum well. In this paper we examine the spin *ejection* process (B), in which spin-polarized carriers are created by optical pumping with circularly polarized light and are then swept out of the semiconductor by the surface depletion field.

ity carriers, which can be achieved by placing a heavily doped *p* layer underneath the *n* layer. Using this approach, Zhu *et al.* recently measured an electroluminescence polarization of approximately 2% in a reverse-biased Fe/GaAs Schottky diode in a perpendicular magnetic field.[7]

The focus of this article is process B of Fig. 1. Although the equilibrium density of states in the semiconductor is not spin polarized, a nonequilibrium population of spin-polarized minority carriers can be created by optical pumping. In this case, the Schottky diode is illuminated with circularly polarized light. The usual selection rules for zinc-blende semiconductors determine the spin polarization of minority carriers that can be achieved by this technique. For photoelectrons in bulk *p*-type GaAs, polarizations very near the theoretical maximum of 50% have been achieved.[8] (The strong spin relaxation of holes makes the optical pumping of minority carriers much less efficient in *n*-type GaAs.) The spin-polarized minority carriers are swept towards the ferromagnet by the depletion field. The question addressed by the experiments discussed in this article is whether the resulting photocurrent is sensitive to the spin-polarized density of states in the ferromagnet.

We have studied a variety of Schottky diode structures grown by MBE on GaAs (100) substrates. All of the samples discussed here are based on $GaAs/In_yGa_{1-y}As$ heterostructures ($y \sim 0.11$). The band gap of $In_yGa_{1-y}As$ at this concentration is $E_g = 1.36$ eV, although it should be noted that the $In_yGa_{1-y}As$ layers in these structures are strained. As will be seen later, the total ground state confinement energy is approximately 60 meV as determined from the absorption spectrum. After growth of the semiconductor structure, each sample was cooled to 95 °C before deposition of the ferromagnet, which was an approximately 200-Å-thick film of Fe or $Fe_{0.5}Co_{0.5}$. X-ray diffraction, Rutherford backscattering, vibrating-sample magnetometery, and magneto-optic Kerr effect measurements indicate films of high crystalline and magnetic quality.[9] Control samples with Al in place of the ferromagnet were also prepared. An overview of the samples is provided in Table I. All of the 100 Å $In_yGa_{1-y}As$ quantum wells were grown on either n^+ or p^+ (10^{18} cm^{-3}) substrates with 1000 Å undoped GaAs barriers on each side of the well. Sample A includes an additional 1000 Å layer of undoped GaAs grown before the ferromagnetic film. Samples D and F contain a 1200 Å *n*-doped (10^{16} cm^{-3}) layer above the quantum well, followed by a Si (10^{12} cm^{-2}) δ-doped layer, 50 Å of undoped GaAs, and the Fe layer. Sample F was made from sample D by removing the Fe layer after growth and evaporating Al in its place.

TABLE I. Details of the samples discussed in this paper. ϕ_b is the Schottky barrier height and *n* is the ideality factor. QW stands for a quantum well of 1000 Å (i)GaAs/100 Å $In_{0.11}Ga_{0.89}As$/1000 Å (i)GaAs, except for samples D and F, where it stands for 500 Å (i)GaAs/100 Å $In_{0.11}Ga_{0.89}As$/500 Å (i) GaAs. Metal layer thicknesses are 200 Å.

Sample	Heterostructure	Metal	ϕ_b (V), *n*
A	i(1000 Å)QW/p/p^+	FeCo	0.62, 1.12
B	QW/p/p^+	Fe	0.50, 1.15
C	QW/n/n^+	Fe	0.80, 1.05
D	i(50 Å)/n δ-doped/QW/p/p^+	Fe	NA
E	QW/p/p^+	Al	0.50, 1.15
F	i(50 Å)/n δ-doped/QW/p/p^+	Al	NA

The samples were patterned into mesas by photolithography and wet etching. The experiments were generally done on strips 200 μm wide and approximately 2 mm long. Contacts to the metal were made by wire bonding, and contacts to the semiconductor were prepared by diffusion of In into the back of the wafer. Samples, A, B, C, and E show typical Schottky-diode behavior with ideality factors less than 1.2. Barrier heights are given in Table I. All of these samples show ordinary photodiode behavior under reverse bias. Samples D and F comprise a heavily-doped Schottky diode back-to-back with a $p-n$ junction diode. The $I-V$ curves in this case are consistent with an extremely leaky Schottky contact in series with a $p-n$ junction. However, samples D and F show ordinary photodiode behavior when the metal is biased at a positive voltage relative to the p^+ substrate. We will call this condition reverse bias with the understanding that it is the $p-n$ junction rather than the Schottky contact itself that is under reverse bias.

A schematic diagram of the experiment is shown in Fig. 2. The configuration is similar to that of Prins *et al.* and Hirohata *et al.*[10,11] Light from a Ti:sapphire or HeNe laser is chopped mechanically, and the helicity is switched between right and left using a photoelastic modulator (PEM). For the first set of experiments discussed here, the light was focused on the top of the Schottky diode, parallel to the applied magnetic field. The photocurrent was measured using a lock-in referenced to the chopper frequency ($\sim$500 Hz), while the difference between the currents under right- and left-circularly polarized excitation was measured simultaneously using a lock-in referenced to the PEM, which runs at 42 kHz. We will focus in the remainder of this article on the polarization signal $\Delta I/I$, which is the ratio of the PEM and chopper signals. The polarization signal is therefore the fraction of the total photocurrent that depends on the helicity of the incident light. It is shown as a function of bias voltage in Fig. 3 for sample B, a *p*-type Schottky diode. The large signal on the left-hand side of the dashed line is an artifact of the device reactance, which produces different phase shifts at the PEM and chopper frequencies when the diode goes into for-

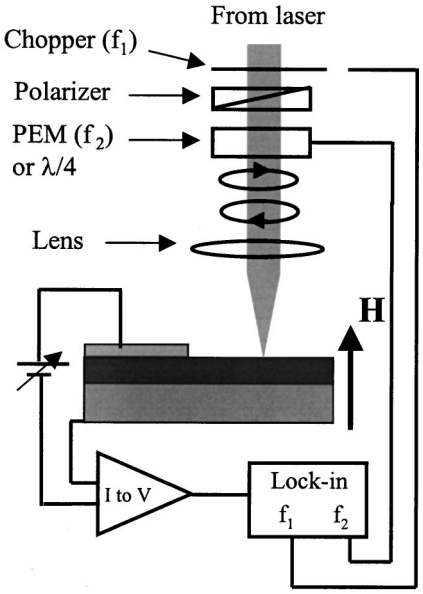

FIG. 2. The experimental setup for the spin ejection measurements. The total photocurrent is measured by a lock-in referenced to the chopper frequency, while the polarization-dependent photocurrent is measured simultaneously by a lock-in referenced to the PEM. The ratio of these signals is the polarization signal $\Delta I/I$.

ward conduction. This regime will not be discussed further in this article.

The field dependence of the polarization signal for sample A at $T=10$ K is shown in Fig. 4 along with the polar Kerr rotation measured on the same sample. It is evident that the observed polarization signal tracks the magnetization of the ferromagnetic film very closely, saturating above 2 T at approximately 3%. This represents an upper bound on the actual spin transport efficiency. Among the various background effects that can mimic spin transport, one of the likely candidates is the differential magnetoabsorption of the ferromagnetic film itself, which would lead to a modulation of the total photocurrent at the PEM frequency, even if spin-dependent transport were completely absent. The magnetoabsorption was measured in a transmission geometry using the same detection electronics as in Fig. 2, with a thinned

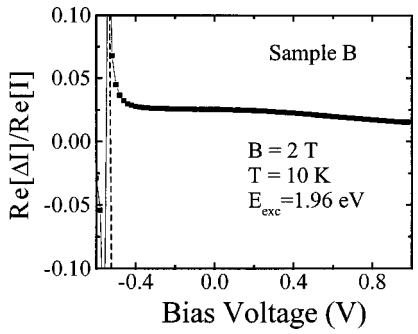

FIG. 3. The real part of the polarization-dependent photocurrent signal divided by the real part of the total photocurrent is shown as a function of bias voltage for sample B. Positive voltages correspond to reverse bias. The apparent rapid increase in the signal when the diode goes into forward conduction (at the dashed line) is an artifact due to the reactance of the device.

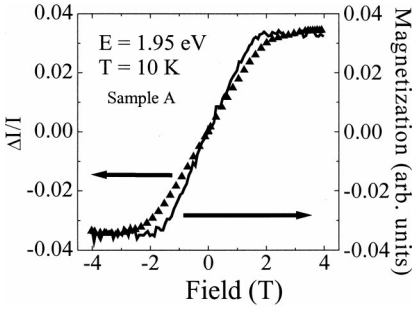

FIG. 4. The polarization signal (triangles) is shown as a function of magnetic field for sample A. The polar Kerr rotation measured on the same sample is shown as the solid curve.

sample and a separate photodetector. The resulting magnetoabsorption closely resembles the polar Kerr data of Fig. 4, with a saturation value of approximately 2.5%.[3] An important question is whether the difference of approximately 0.5% between the magnetoabsorption data and the photocurrent polarization signal is physically meaningful. In order to establish this, it is necessary to prove that the response of the Schottky photodiode is linear in the small 42 kHz modulation that is generated by the magnetoabsorption in the ferromagnetic film. A set of polarization optics was set-up that mimicked the experimental condition: a small circularly polarized component, modulated at 42 kHz, superimposed on the chopper signal. We found that the relative signal $\Delta I(42\ \text{kHz})/I_{\text{Chopper}}$ in this case was linear in the magnitude of the 42 kHz component and identical to the same ratio measured using a commercial photodiode. Hence, approximately 0.5% of the polarization signal in Fig. 4 cannot be attributed solely to the magnetoabsorption in the $Fe_{0.5}Co_{0.5}$ film and may be due to spin-dependent transport.

Given the fact that the magnetoabsorption and photocurrent polarization signals are so close in magnitude, we investigated other means of isolating a spin-dependent transport signal. One approach is varying the bias voltage. Figure 5(a) shows the polarization signal as a function of bias voltage for sample D at several magnetic fields. This sample is *p* type, and so positive voltages correspond to reverse bias. The saturation with field seen above in Fig. 4 is clearly evident, but it is also apparent that the saturation value depends on bias voltage. In Fig. 5(b) we show the polarization signal as a function of magnetic field at several different bias voltages. The difference of the field-dependent signals at 1.5 and 0 V is shown below the dashed line, and it also tracks the magnetization of the ferromagnetic film. In this case, however, control measurements similar to those in the preceding paragraph were also carried out, and we have found that the relative sensitivity to a 42 kHz modulation signal depends on the bias voltage, and the scale of the effect (approximately 20% of the total signal over the range of bias voltages shown in Fig. 5) is comparable to the shift seen in Fig. 5(b). As a result, we cannot claim that the subtraction procedure carried out in Fig. 5 removes magnetoabsorption effects entirely.

If the HeNe laser is replaced by a Ti:sapphire laser, the excitation energy can be tuned down through the band gap of GaAs. This reduces the kinetic energy of the excited photo-

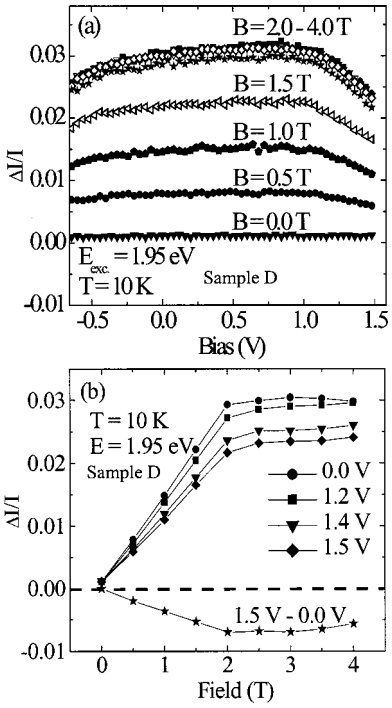

FIG. 5. (a) The polarization signal for sample D is shown as a function of bias at several different magnetic fields, in intervals of 0.5 T. (Positive voltages correspond to reverse bias.) (b) The polarization signal as a function of magnetic field is shown for several different bias voltages. Subtracting the 0 V data from the 1.5 V data yields the points shown below the dashed line.

carriers, allowing for optical pumping efficiencies near the theoretical maximum of 50% for *p*-type GaAs. The polarization signal for sample D at 2 T is shown as a function of energy for several different bias voltages in Fig. 6. The prominent Landau oscillations in these data are due to the magnetoabsorption in the semiconductor. These also produce a background contribution to the polarization signal that can be removed in part by subtracting data at different bias voltages using the procedure described in the previous paragraph. The magnitude of the subtracted signal increases as the band edge is approached from above, but the saturation of the field dependence (not shown) becomes less pronounced. Unfortunately, in this regime there are three significant background contributions: (1) magnetoabsorption in the ferromagnetic film, (2) magnetoabsorption in the semiconductor, and (3) the bias dependence of the photocurrent sensitivity. Under these conditions, it is not possible to establish a rigorous lower bound on the spin transport coefficient.

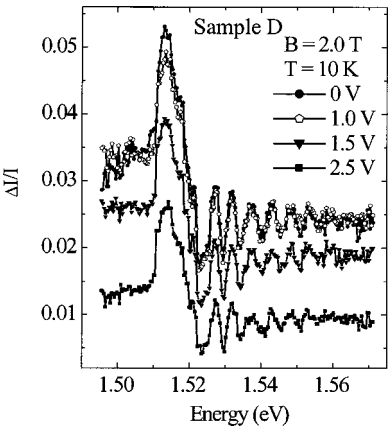

FIG. 6. The spectral dependence of the polarized signal for sample D in the vicinity of the band gap of GaAs, for several values of the bias voltage. Note the decrease in the amplitude of the signal at large bias.

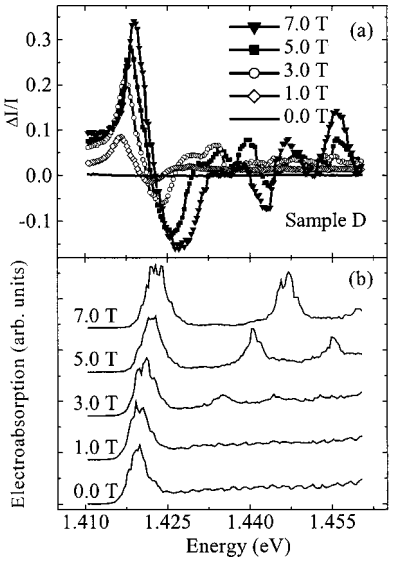

FIG. 7. (a) The spectral dependence of the polarized photocurrent signal for sample D at several magnetic fields. (b) The corresponding electroabsorption data, offset for clarity, showing the large quantum well ground state peak and a series of field-dependent peaks attributed to Landau levels.

Given the data of Figs. 4–6 and the background effects discussed earlier, we estimate an upper bound of approximately 0.5% for the spin polarization of the photocurrent at excitation energies above the GaAs band edge. This motivated us to investigate excitation energies near the ground state of the $In_yGa_{1-y}As$ quantum well. Figure 7 shows the electroabsorption and polarization spectra for sample D in several different magnetic fields at $T=10$ K. The prominent peak at the lowest energy in Fig. 7(b) corresponds to the ground state exciton, and the peaks fanning out at higher energies in magnetic field are attributed to Landau levels. The polarization spectra shown in Fig. 7(a) show much larger effects than observed for excitation energies above the GaAs band edge. The largest polarization signal measured at the ground state peak is 35% in a field of 7 T.

The dominant contribution to the peaks in the polarization spectrum of Fig. 7(a) comes from the magnetic circular dichroism (MCD) of the quantum well, which is extremely sensitive to the Zeeman splitting of the density of states.[12] There is also a weak energy-independent background of approximately 2% due to the magnetoabsorption in the ferromagnetic film. Modulating the bias voltage was not a useful approach in the quantum well regime because the density of states is itself a strong function of the bias voltage, which leads to a substantial Stark shift. As a result, it is not possible to examine the field dependence at fixed energy by subtracting data obtained at different biases. (The spectra shown in Fig. 7 were obtained at a small forward bias voltage at which the bands near the quantum well were approximately flat.)

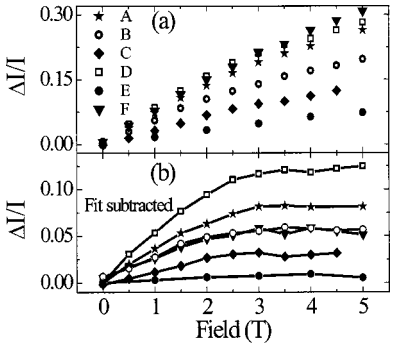

FIG. 8. (a) The maximum value of the polarized photocurrent at the quantum well ground state exciton is shown as a function of magnetic field for all of the samples in this study. (b) The same data are shown after the subtraction of a background determined by fitting the data of (a) to a straight line above 3 T.

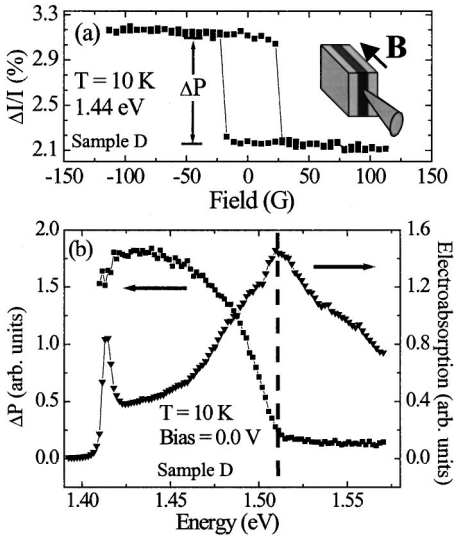

FIG. 9. (a) The polarization signal as a function of magnetic field for sample D in the side-pumping geometry shown in the inset. We define the shift ΔP to be the difference in the polarization signals measured at the two endpoints of the hysteresis loop. (b) ΔP (squares) is shown as a function of excitation energy along with the total electroabsorption signal (triangles). The dashed line indicates the GaAs band edge.

Another scheme for removing the background MCD is suggested by the observation that if it is due to the splitting of a single quantum well level, then the MCD should be linear in applied field. The magnitude of the ground state polarization peak is shown as a function of field in Fig. 8(a) for all of the samples we have studied. Above 2 T, where the ferromagnetic film is saturated, the polarization signals do depend linearly on field, and we proceed with our analysis by assuming that the slope of the high-field data is due to the background MCD. The data of Fig. 8(b) are obtained from those of Fig. 8(a) by subtracting off a linear fit of the high-field polarization signal data for each sample.

There are several features of the data in Fig. 8(b) that are suggestive of a spin-dependent photocurrent. With the exception of the completely nonmagnetic control sample E, the curves show the saturation expected for the ferromagnetic electrode. It is important to note that the *p*-type samples show the largest polarization signal. Since the photocarriers in this case are electrons, for which spin scattering is much weaker than for holes,[13] we expect the polarization signals to be largest in *p*-type samples and smallest in *n*-type ones, such as sample C. This will be true if the time-scale for carriers to escape from the quantum well is on the order of the spin lifetime.

Given a background of order 2% from the MCD of the ferromagnetic film, the largest spin transport coefficient that can be inferred from the data of Fig. 8(b) is approximately 10% for sample D. However, the behavior of sample F, which was prepared from sample D by removing the Fe film and then evaporating Al in its place, is not consistent with a spin transport picture. We expected the polarization signal from sample F to be essentially zero after the linear background was subtracted, as was observed for sample E, in which the Al film was grown *in situ*. Although the polarization signal for sample F is smaller than found for sample D, it is still over 5% and also appears to saturate in a similar manner to the magnetic samples. We considered the possibility that some of the ferromagnetic film remained on the surface after etching, but Auger spectroscopy shows no detectable Fe. Given this observation, the data of Fig. 8(b) must be regarded as suggestive of spin transport but not conclusive. The assumption of a linear dependence for the quantum well MCD is certainly subject to challenge.

The Faraday geometry used for the measurements discussed earlier, in which both the direction of the incident light as well as the magnetic field are along the sample normal, offers one great advantage when using the quantum well as a generator of spin: the optical selection rules provide for a direct mapping between the degree of circular polarization and the spin state of the photocarriers. For wells with a large heavy-hole/light-hole splitting, the theoretical optical pumping efficiency is 100%. However, saturation of the ferromagnetic films, which have a large moment and correspondingly large shape anisotropy energy, requires the application of magnetic fields in excess of 2 T. These fields are sufficient to generate the background effects discussed earlier, particularly the MCD observed in the quantum well measurements and the magneto-oscillations that occur for excitation energies near the GaAs band gap. The use of a ferromagnetic material with an easy axis perpendicular to the film plane would avoid this problem. Another approach, which comes at the cost of complicating the usual selection rules, is to pump the heterostructure from the side, as shown in the inset of Fig. 9(a). Since the coercitivities of our ferromagnetic films are less than 100 Oe, only small fields are required to reverse the magnetization of the ferromagnet, and the MCD effects discussed earlier are therefore eliminated.

The polarized photocurrent signal measured as a hysteresis loop is traced in the side-pumping geometry is shown in Fig. 9(a) for an excitation energy of 1.44 eV. The magnetic hysteresis is clearly visible, and the total change in the signal between -100 and $+100$ Oe is 1% of the total photocurrent. There are several features of the side-pumping measurements that are very different from pumping at normal incidence. First, there is no hysteresis signal at excitation energies above the band gap (1.5 eV). Even if the sample is deliber-

ately misaligned so that some light leaks in through the top of the ferromagnetic layer, only a very weak ($<0.1\%$) hysteresis signal is observed at an excitation energy of 1.95 eV. Interestingly, the sign of the signal in Fig. 9(a) is opposite to that observed when light enters through the top of the heterostructure. We emphasize that although we observe no hysteresis signal when we pump above band gap in the side-pumping geometry, there is still a photocurrent, as can be seen in Fig. 9(b), which shows the total change ΔP in the polarization signal between the endpoints of the hysteresis loop (left axis) and the total photocurrent (right axis). Another interesting feature of these data is that there is no longer a maximum in the polarization signal at the quantum well ground state. In contrast, the polarization signal in Fig. 9(b) starts to fall off at energies *above* the quantum well absorption peak. This is consistent with the selection rules for this geometry, which prohibit optical pumping of electron spins from the heavy-hole valence states. The confined spin is locked along the growth direction by the spin-orbit interaction. Mixing of the heavy and light-hole states at nonzero in-plane wave vectors leads to a breakdown of the selection rules at higher energies, and this may be why a hysteresis signal is observed at energies between the quantum well (QW) ground state and the GaAs band edge. More detailed magneto-optical spectroscopy is required to address the important role of the selection rules in determining the absolute size of the polarization signal in the measurements presented here as well as in polarization-resolved electroluminescence experiments.

This article has reviewed the fundamental phenomenology of optically pumped transport in ferromagnet-semiconductor Schottky diodes. It is evident that a systematic investigation as a function of several parameters, including magnetic field, excitation energy, bias dependence, and excitation geometry, is necessary to isolate background effects that may mimic or mask spin-dependent transport. The spin-dependent fraction of the photocurrent is at most 0.5% for excitation energies above band gap and is at most 10% for ground-state excitation of *p*-type quantum well samples. In concluding, it should be emphasized that obtaining a spin-dependent photocurrent from the type of measurement introduced here relies on two factors: (1) a spin-dependent transmission coefficient at the ferromagnet-semiconductor interface, and (2) efficient recombination of the reflected minority spin carriers in the semiconductor, so that they do not simply bounce back and eventually enter the ferromagnet. Unfortunately, these conditions make a quantitative prediction of the spin-dependent photocurrent difficult to achieve, even for an ideal interface. In contrast, the analysis of spin injection through a tunneling barrier is relatively straightforward, although a detailed study of the relaxation of the injected spin-polarized carriers will need to be undertaken. The measurements presented here will be useful in understanding the distinctions among these possible spin transport processes, particularly since the experimental interpretation relies to such a great extent on knowledge of magneto-optical effects.

This work was supported by DARPA/ONR-N/N00014-99-1005, ONR N/N00014-99-1-0233, NSF MRSEC 98-09364, and the Alfred P. Sloan Foundation (PAC).

[1] P. C. van Son, H. van Kempen, and P. Wyder, Phys. Rev. Lett. **58**, 2271 (1987).
[2] G. Schmidt, D. Ferrand, L. W. Molenkamp, A. T. Filip, and B. J. van Wees, Phys. Rev. B **62**, R4790 (2000).
[3] A. F. Isakovic, D. M. Carr, J. Strand, B. D. Schultz, C. J. Palmstrom, and P. A. Crowell, Phys. Rev. B **64**, 161304R (2001).
[4] R. Fiederling *et al.*, Nature (London) **402**, 787 (1999).
[5] Y. Ohno *et al.*, Nature (London) **402**, 790 (1999).
[6] B. T. Jonker *et al.*, Phys. Rev. B **62**, 8180 (2000).
[7] H. J. Zhu *et al.*, Phys. Rev. Lett. **87**, 016601 (2001).
[8] M. I. Dyakonov and V. I. Perel, in *Optical Orientation*, edited by F. Meier and B. P. Zakharchenya (North-Holland, Amsterdam, 1984), p. 11.
[9] L. C. Chen *et al.*, J. Vac. Sci. Technol. B **18**, 2057 (2000).
[10] M. W. J. Prins *et al.*, J. Phys.: Condens. Matter **7**, 9447 (1995).
[11] A. Hirohata *et al.*, Phys. Rev. B **63**, 104425 (2001).
[12] D. M. Hofmann, K. Oettinger, A. L. Efros, and B. K. Meyer, Phys. Rev. B **55**, 9924 (1997).
[13] G. E. Pikus and A. N. Titkov, in *Optical Orientation*, edited by F. Meier and B. P. Zakharchenya (North-Holland, Amsterdam, 1984), p. 73.